

Intermolecular Potential Function for Hydroxylamine Dimer Interactions from *ab initio* Calculations

Yanos Michopoulos¹, Peter Botschwina², and Bernd M. Rode¹

¹ Institute for Inorganic and Analytical Chemistry, University of Innsbruck, Innrain 52a, A-6020 Innsbruck, Austria

² Theoretical Chemistry, University of Kaiserslautern, D-6750 Kaiserslautern, Germany

Z. Naturforsch. **46a**, 32–38 (1991); received June 29, 1990

Dedicated to Dr. K. Heinzinger on the occasion of his 60th birthday

The derivation of an intermolecular potential function for the interaction of two hydroxylamine molecules, based on *ab initio* SCF-ECP calculations is reported. *Ab initio* values were compared for selected geometries with those obtained from calculations with much larger basis sets, including electron correlation effects by the CEPA method. A total 658 energy values were then fitted to an analytic sum of atom-atom isotropic pair potential functions, whose functional form was given a simple electrostatic interpretation. The major difficulties, arising from the relatively low values of the stabilisation energies of the system and the numerous possibilities to form hydrogen bonds, were overcome by a careful selection of sufficient points on the potential hypersurface, introduction of cut-offs and weight factors. The obtained function was seen to be able to give a good reproduction of the interaction energies and proved suitable in a preliminary MC simulation.

1. Introduction

For the computer simulation of liquids [1], realistic pair potentials between the molecules involved are needed.

In this note we report the construction of a potential function for the interaction between two hydroxylamine molecules based on *ab initio* SCF calculations. Hydroxylamine has been chosen for several reasons. First, being still a relatively small molecule, it allows the application of sufficient accurate *ab initio* calculations. Second, chemically situated between water and ammonia [2] and being a good solvent for electrolytes, MC and/or MD simulations of ions in hydroxylamine as solvent will be of particular interest for comparisons with similar simulations for water [3], ammonia [4] and water/ammonia mixtures [5] as solvents. Third, the possibility of forming several types of hydrogen bonds and the existence of two possible coordination sites for ions make this molecule an especially versatile and challenging example for a theoretical approach, as experimental methods for structural investigations of hydroxylamine solutions meet several restrictions that could be overcome by the quantum chemical and statistical simulation treatment.

Reprint requests to Prof. Dr. B. M. Rode, Institut für Anorg. und Analytische Chemie, Universität Innsbruck, Innrain 52a, A-6020 Innsbruck, Österreich.

2. Method

2.1. Monomer Geometry and Basis Set

As a first step, full geometry optimisations by the force field method have been carried out for hydroxylamine with various basis sets. As the results collected in Table 1 show, considerably diverging data are obtained, and even the best of these standard basis sets do not lead to full agreement with experimental data [6]. Moreover, it could be expected from results for hydrogen peroxide and hydrazine [7], that electron correlation will be a non-negligible factor for the determination of the equilibrium geometry, especially the N–O bond length [8]. This influence of electron correlation on geometry optimization was studied at CEPA-level using a relatively large basis set [9] of 90 contracted GTO's: 11 s/6 p/2 d contracted to 8 s/4 p/2 s for N and O and 6 s/2 p to 4 s/2 p for the H's. Only at this level of accuracy, satisfactory values for all geometrical parameters could be obtained (cf. Table 1).

However, due to the enormous computational effort required for such calculations even in case of the monomer, a full energy surface evaluation at this level is not feasible yet. Instead, for a HF-level evaluation of the intermolecular interaction between two hydroxylamines, the following procedure was employed: As it is also shown in Table 1, employment of the ECP approximation [10] with a double zeta + polarization

0932-0784 / 91 / 0100-0032 \$ 01.30/0. – Please order a reprint rather than making your own copy.



Dieses Werk wurde im Jahr 2013 vom Verlag Zeitschrift für Naturforschung in Zusammenarbeit mit der Max-Planck-Gesellschaft zur Förderung der Wissenschaften e.V. digitalisiert und unter folgender Lizenz veröffentlicht: Creative Commons Namensnennung-Keine Bearbeitung 3.0 Deutschland Lizenz.

Zum 01.01.2015 ist eine Anpassung der Lizenzbedingungen (Entfall der Creative Commons Lizenzbedingung „Keine Bearbeitung“) beabsichtigt, um eine Nachnutzung auch im Rahmen zukünftiger wissenschaftlicher Nutzungsformen zu ermöglichen.

This work has been digitalized and published in 2013 by Verlag Zeitschrift für Naturforschung in cooperation with the Max Planck Society for the Advancement of Science under a Creative Commons Attribution-NoDerivs 3.0 Germany License.

On 01.01.2015 it is planned to change the License Conditions (the removal of the Creative Commons License condition "no derivative works"). This is to allow reuse in the area of future scientific usage.

Table 1. Geometry optimization for different basis sets.

| Basis set | Bond | Length (Å) | | Angle (degree) | | Energy (Hartree) |
|----------------------|-------|------------|-------|----------------|-------|------------------|
| | | N–O | O–H | HNH | HON | |
| GLO ^a | 1.194 | 1.585 | 1.109 | 92.2 | 92.2 | –111.39 |
| STO-3G | 1.044 | 1.427 | 0.995 | 103.4 | 101.3 | –129.26 |
| 8s 4p | 1.048 | 1.631 | 1.086 | 102.1 | 103.2 | –124.89 |
| STO3-21G | 1.009 | 1.469 | 0.967 | 109.2 | 103.4 | –130.26 |
| STO4-31G | 0.998 | 1.442 | 0.952 | 111.4 | 106.0 | –130.79 |
| DZV ^b | 1.000 | 1.431 | 0.952 | 111.9 | 107.0 | –130.96 |
| DZP ^b | 1.002 | 1.400 | 0.943 | 107.3 | 104.6 | –131.03 |
| TZV ^b | 0.999 | 1.430 | 0.951 | 111.5 | 104.3 | –130.98 |
| TZP ^b | 0.999 | 1.399 | 0.940 | 107.6 | 104.8 | –131.04 |
| DZV/ECP ^c | 1.004 | 1.434 | 0.956 | 111.6 | 106.6 | –27.003 |
| DZP/ECP ^c | 1.006 | 1.405 | 0.946 | 107.0 | 104.4 | –27.063 |
| TZP/ECP ^c | 1.001 | 1.434 | 0.952 | 111.4 | 106.5 | –27.032 |
| DZP/ECP ^d | 1.005 | 1.406 | 0.946 | 106.9 | 104.5 | –27.052 |
| CEPA, 90cGTO's | 1.013 | 1.449 | 0.957 | 105.2 | 103.5 | –131.50 |
| CEPA, 60cGTO's | 1.017 | 1.453 | 0.960 | 105.0 | 101.8 | –131.46 |
| Exp. ^e | 1.017 | 1.453 | 0.962 | 107.1 | 101.4 | – |

^a Ref. [17]. – ^b Ref. [18]. – ^c Ref. [10]. – ^d As in [10] but with polarization functions on N and O only. – ^e Ref. [6], obtained by fitting to rotational constants.

Table 2. Optimized geometry for hydrogen-bonded dimers (for their definition refer to Figure 1).

| Geometry | Bond length (Å) | Angle (degree) | ΔE (kcal/mol) |
|----------|-----------------|----------------|-----------------------|
| OH...O | O...O = 2.99 | NO–O = 135 | –4.13 |
| OH...N | O...N = 3.03 | ON–O = 60 | –4.61 |
| CYC | O...N = 3.01 | NO–O = 60 | –8.58 |
| NH...O | N...O = 3.25 | N–ON = 205 | –2.50 |
| NH...N | N...N = 3.40 | ON–N = 125 | –2.37 |

basis set for the heavy atoms only could be seen as an acceptable compromise between computational effort and accuracy.

The validity of this basis set for calculating dimer interaction energies when compared to the more accurate SCF and CEPA results also holds, using the rigid experimental geometry of the monomer and calculating the stabilization energies of some important hydrogen bonded dimers: Results collected in Table 2 show that, although absolute energies values are not very accurate, the relative order of stability for the various dimers is rather well preserved. This hierarchy of stabilization energies should also be a very important feature for a subsequent simulation study and represents therefore a rigorous test for the quality of the potential function. It should also be noted that the difference of the SCF energies for the basis sets can give a rough estimate of the basis superposition error

[11] (in the region of 2–5%). From this analysis, it could be expected that use of the ECP-DZP basis set could lead to a reasonably accurate description of the energy hypersurface of the hydroxylamine-hydroxylamine interaction and hence form the basis for the derivation of a reliable intermolecular potential function.

2.2. Selection of Dimer Geometries

For a complete representation of the potential hypersurface, the two interacting hydroxylamine molecules should be placed at different distances apart and at different relative orientations. Keeping the first molecule fixed, the exact position of the second molecule is determined by three translational parameters (r, ϑ, ϕ) between two specified atoms in each molecule (say the two oxygens) and three internal rotations (α, β, γ) with respect to the reference axes of coordinates. Despite the fact that some of these configurations are symmetry-related due to the C_s symmetry of the hydroxylamine monomer, the task to perform energy calculations for points on a complete grid on this 6-dimensional space is computationally not feasible. Instead, energy points had to be calculated only for a representative subset of points, which contained the following configurations.

a) Hydrogen bonded configurations (see Fig. 1) which are of chemical importance, containing local and absolute minima of the potential hypersurface. Such minima were located by selecting an appropriate relative orientation of the second hydroxylamine molecule (values of α, β, γ) and searching for an energy minimum in the $r-\vartheta$ subspace (Table 2).

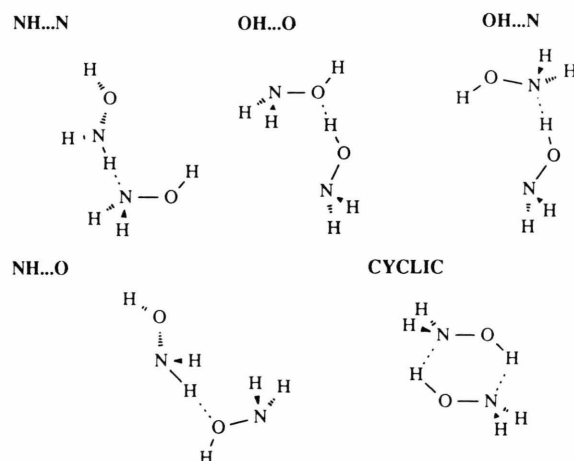


Fig. 1. Hydrogen-bonded hydroxylamine dimers.

b) Trajectories generated with the O(2) atom on the C_s symmetry plane ($\phi = 90^\circ$) and the second molecule in three different internal planes (xy , yz , and zx , respectively). These trajectories span the r -range from 2 to 7 Å for various ϑ -angle choices ($0^\circ < \vartheta < 360^\circ$ in steps of 45°).

c) Trajectories similar to the ones described above, but with the O(2) atom lifted out of the symmetry plane and different relative orientations of the second molecule: In particular two cases were considered: (i) $\phi = 45^\circ$ with the second molecule's plane at 45° and 135° respectively, relative to the first molecule's plane and (ii) $\phi = 0^\circ$ with the second molecule in one of the three reference planes xy , yz , and zx .

This subset of configurations gave 658 energy points on the potential hypersurface, with energies less than +50 kcal/mol. Calculations were performed using version 7 of the HONDO program [12] and required between 500 and 1500 CPU second on the CYBER-840 of Innsbruck University.

2.3. Choice of Potential Function and Fitting Method

The calculated SCF energies for the above mentioned configurations were then fitted to an analytic potential function of the atomic coordinates. We assumed pair-wise additivity, so that the total intermolecular interaction energy was written as a sum of atom-atom pair potentials, each of which was considered to be an isotropic function of the distance R_{ij} of the two atoms concerned, that is

$$U_{\text{intermolec}} = \sum_i \sum_j U_{ij}(R_{ij}), \quad \begin{array}{l} i: \text{ in first molecule} \\ j: \text{ in second molecule} \end{array} \quad (1)$$

Of course the true intermolecular potential function is unknown, but the functional form of the pair potentials U_{ij} was chosen with a physical model in mind: there should be a term to describe the Coulombic interaction between the atom pairs, and the Mulliken population analysis of the ab initio calculations was used to get a first estimate of the fractional atomic charges. Then, additional terms of the form B/R_{ij}^m , $m = 2 \dots 6$, especially effective at medium distances, should be added to describe phenomena like the distance dependence of these charges, and the mutual disturbance of the charge distributions which results in induced dipole moments and their interaction with the above points charges as well as between them. Finally, there should be a term to represent the electronic repulsion at close distances and take care of

the Pauli exclusion principle, which effect increases nucleonic repulsion. This term is typically represented by either a polynomial R^{-n} , $n = 8 \dots 15$ or an exponential $\exp\{-R_{ij}\}$ functional. Therefore a trial potential function U_{ij} was set up as

$$\Delta U_{ij}(R_{ij}) = A_{ij}/R_{ij}^n - B_{ij}/R_{ij}^m + C_{ij} Q_i Q_j / R_{ij} \quad (2)$$

with the coefficients A_{ij} , B_{ij} , and C_{ij} to be determined so that a best fit to the SCF calculated energies is achieved. However, it should be emphasized that these coefficients should be treated with some care and not only as mathematical objects, especially if the obtained potential is to be used in a subsequent simulation study. For instance, negative values for the A_{ij} coefficients may result in the corresponding atomic potential function turning negative at very small distances, and an arbitrary choice of the C_{ij} coefficients may not reproduce the correct limit of the electrostatic energy at large distances.

The fitting procedure was carried out by minimizing the sum of squared differences between the SCF calculated energies and those given by the trial potential function, with respect to the potential parameters. The minimization itself was based on a multidimensional non-linear Marquard-Levenberg algorithm, which changes softly from an initial steepest descent to a quadratic approximation of the potential parameters near the minimum. To improve the quality of the fit, especially in the most important configurations (which correspond to the lowest lying values of the SCF energy points) additional weight factors were introduced, and very repulsive configurations (with positive energy values larger than +50 kcal/mol) were excluded from the process.

2.4. Testing the Function

The quality of the fit for the obtained potential function was judged by its statistical characteristics (standard deviation, residuals etc.), the values and positions of energy minima for the chemically important configurations, and a graphical representation of fitted energies vs. their quantum mechanically calculated values. Moreover, the "predictive" capabilities of the potential function were then tested according to the procedure suggested by Beveridge *et al.* [13]. Namely, the SCF energies for 20 additional configurations (outside the original set) were calculated and compared with the values predicted by the function. These points were then included in the fitting proce-

ture and the whole process was repeated until satisfactory results were obtained (details in next section).

3. Results and Discussion

For the fractional atomic charges obtained by Mulliken population analysis it was observed that in each of the two interacting molecules they have to a first approximation the same values as in the monomer (cf. Table 3). Following this observation, and in accordance with standard fitting procedure [14], atomic charges were assigned their monomer values and were kept fixed during the fitting process. Remaining charge fluctuations should be taken care of by the middle r^{-m} terms. Consequently, all parameters C_{ij} for the Coulombic term of the pair potentials were set to 1.

It should be noted here that usage of the monomer charges obtained by a Mulliken population analysis of our SCF calculations resulted in a relatively large molecular dipole moment of 1.16 D, compared to both the SCF value (0.82 D) and the experimental one (0.59 ± 0.05 D) [6]. Realistic estimates for the dipole moment could only be obtained at the CEPA level (0.596 D).

For the repulsive and attractive terms of the potential function (2), a number of combinations for the (n, m) pair of exponents were tried, including the possibility of different exponents for different atom-atom pairs. It was then found that the optimal functional form which ensured both positive definite values for the A_{ij} coefficients of all pair potentials and good overall fitting results, was characterized by a $(n, m) = (9, 3)$ choice. These exponents can be understood in the light of the following remarks:

R^{-3} can be seen as representing the interaction between a fractional atomic charge on one molecule

and an induced dipole moment on a atomic site of the second molecule: as the second molecule approaches the first one, its atomic charges, and in particular the one of the atom nearest to the first molecule, should disturb the atomic charge distribution of the first molecule, creating small dipole moments on every atomic site, which are of course proportional to the field responsible for their formation, namely the $1/r$ field of atomic sites of second molecule. These dipole moments create their own local electric field, varying as $1/r^2$, which would then interact with the atomic charges of the second molecule, thus giving rise to the overall $1/r^3$ term for the total potential function. It should be remembered though, that this is an angular dependent interaction, but this angular dependence is seen to be somehow averaged out in the final value and sign of the B_{ij} coefficients. These induced atomic moments will in turn disturb the atomic charges of the first molecule creating dipole moments there as well and giving rise to the ever popular R^{-6} term for an induced dipole-induced dipole interaction. However, in an atom-atom interaction picture, R^{-3} should be the leading term of the multi-dipole expansion, whereas R^{-6} would have been the leading term in a single intermolecular potential function describing the interaction of two neutral molecules. For similar reasons, there should be no R^{-2} term, as this would have implied the existence of permanent dipole moments on the atomic sites. R^{-3} terms for the atom-atom pair potential have been used quite extensively in developments of potential models for molecular systems [13, 15].

The $n=9$ choice for the repulsive part of the potential was simply determined by the fitting procedure itself. We compared not only standard deviations for different choices (considering all possibilities in the interval $n=8, 15$ as well as an exponential term) but also checked the quality of the fit for individual energy curves, and in particular those which corresponds to the chemically most important configurations (see Figs. 1, 2 and Table 4), for which we had to maintain their relative hierarchy of stabilization energies.

In fact, the latter requirement has often caused potential functions of relatively high values for their total standard deviations to be preferred over those of lower values. Moreover, the position and shape of the fitted function near the local energy minima has also been seen to be of crucial importance in computer simulations. It was then reassuring to observe that our minima in those curves were not shifted

Table 3. Fractional atomic charges for different hydrogen-bonded configurations.

| Atom | Mono | CYC | OH...O | OH...N | NH...O | NH...N |
|------|-------|-------|--------|--------|--------|--------|
| HO1 | .405 | .438 | .424 | .408 | .400 | .405 |
| HO2 | .438 | .434 | .434 | .434 | .417 | .401 |
| O1 | -.525 | -.523 | -.567 | -.503 | -.534 | -.510 |
| O2 | | -.523 | -.545 | -.547 | -.553 | -.535 |
| N1 | -.482 | -.543 | -.463 | -.535 | -.493 | -.514 |
| N2 | | -.543 | -.484 | -.489 | -.467 | -.494 |
| HN1 | .301 | .314 | .306 | .322 | .332 | .315 |
| HN2 | .301 | .314 | .307 | .322 | .290 | .311 |
| HN3 | | .314 | .293 | .294 | .303 | .291 |
| HN4 | | .314 | .293 | .294 | .306 | .331 |

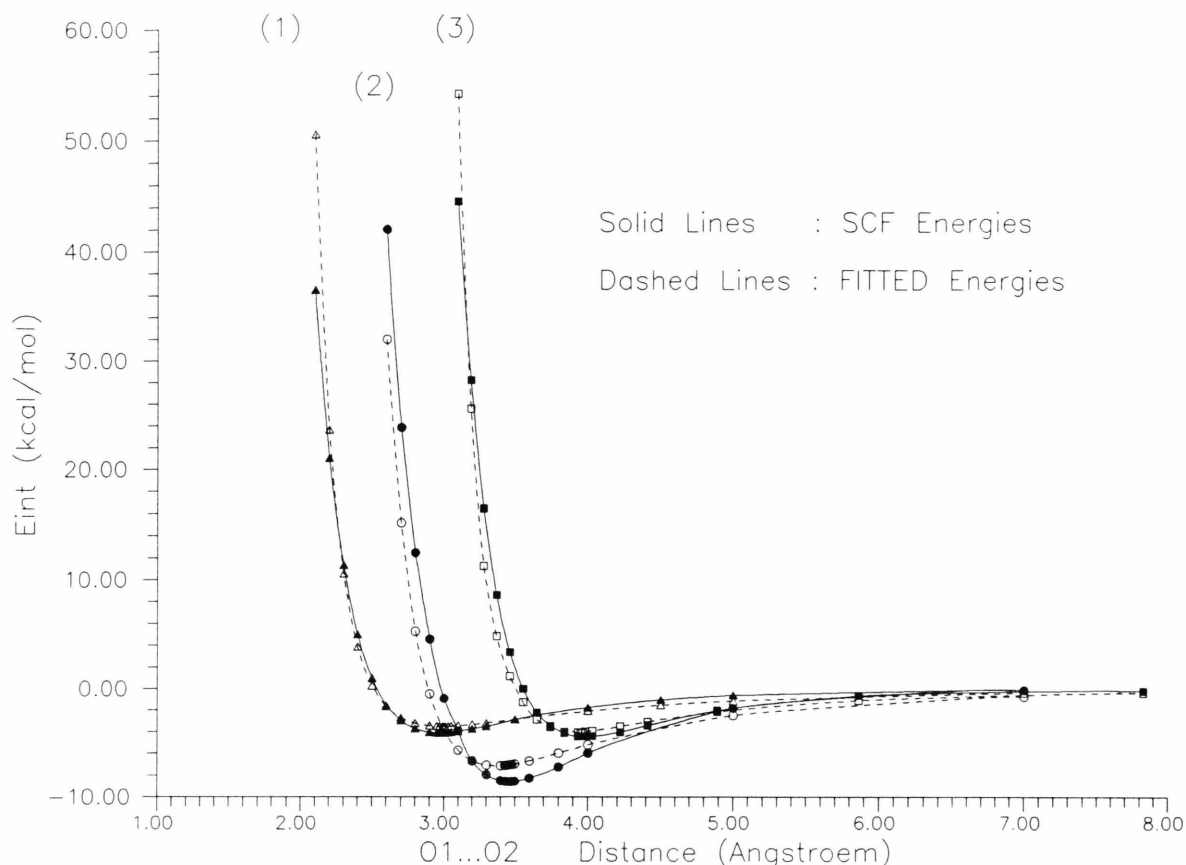


Fig. 2. SCF calculated and potential fitted energy curves for the three lowest lying hydrogen-bonded dimers: (1) $\text{OH} \cdots \text{O}$, (2) CYC, (3) $\text{OH} \cdots \text{N}$.

Table 4. Stabilization energies and their ratios with respect to the $\text{OH} \cdots \text{O}$ energy value for different hydrogen-bonded configurations.

| Energies (kcal/mol) | $\text{OH} \cdots \text{O}$ | $\text{OH} \cdots \text{N}$ | CYC | $\text{NH} \cdots \text{O}$ | $\text{NH} \cdots \text{N}$ |
|--|-----------------------------|-----------------------------|--------|-----------------------------|-----------------------------|
| SCF (DZP/ECP) ¹ | -4.13 | -4.46 | -8.58 | -2.50 | -2.37 |
| SCF (90 contracted GTO's) ¹ | -3.89 | -4.39 | -8.38 | — | — |
| CEPA (90 contracted GTO's) ¹ | -4.86 | -5.94 | -11.21 | — | — |
| Fitted values | -3.61 | -4.13 | -7.14 | -2.08 | -1.95 |
| Ratios (w.r.t. $\text{OH} \cdots \text{O}$) | | | | | |
| SCF (DZP/ECP) | 1.00 | 1.08 | 2.08 | 0.61 | 0.57 |
| CEPA | 1.00 | 1.12 | 2.31 | — | — |
| Fitted ratios | 1.00 | 1.14 | 1.98 | 0.58 | 0.54 |
| Difference relative to SCF | | (5%) | (5%) | (5%) | (5%) |

¹ For basis sets definitions refer to text (Section 2.1).

more than 0.05 \AA . The least satisfactory point was the shift of the global minimum towards slightly shorter distance for this (cyclic) dimer (Figure 2). This point will be discussed once more below.

Further, a systematic analysis of all distances between all atoms in the original subset of points revealed certain distance gaps, and in particular a shortage of short distances between certain atom pairs. Therefore, additional configurations were added to our set of calculated points to ensure a more or less uniform distribution of distances.

Finally, in order to achieve a closer representation of the lowest lying values of the dimerisation energy (especially for the hydrogen bonded configurations) it was necessary to introduce additional weight factors for these points according to the formula

$$\text{Weight} = 1/\text{abs}(\text{SCF energy} - \text{YL})^p. \quad (3)$$

YL and p were then fine-tuned for optimum quality for to the following values: $YL = -5.3$ kcal/mol and $p = 1.35$, so that most attractive configurations (lowest energy values) get considerably more weight than the most repulsive ones (highest energy values). This choice also ensured that the relative order and ratios of values for the stabilisation energies of the various hydrogen bonded configurations were maintained to an accuracy of about 5% (Table 4).

3.1. Evaluation and Testing of the Function

According to the iterative procedure outlined in Sect. 2, the predictive power of the potential function was tested by comparing sets of energy values (SCF-calculated and function-predicted) for additional configurations, outside the initial sample. As expected, standard deviations for test sets (Table 5) were always larger than initial sets but still within acceptable limits (less than 10% of the global energy minimum), and gradually improving. This procedure was stopped when negative values for the A_{ij} coefficients were obtained. The final values for all potential parameters are presented in Table 6. Statistical parameters have certainly only relative significance, but a further illustration of the quality of the potential function is shown in Fig. 3, where SCF energies are plotted against fitted values. Perfect agreement would have

Table 5. Standard deviations of potential fitting: a) For different sets of points and test point sets (see text: Sects. 2.4 and 3.1). b) For different energy regions (subsets of the full point set).

| a) Set of points | N_{points} | σ (kcal/mol) | % (E_{min}) | $\sigma_{\text{test}}/\sigma_{\text{set}}$ |
|--------------------|---------------------|---------------------|------------------------|--|
| N_1 | 658 | 0.524 | 6.1 | |
| $N_{\text{test}1}$ | 20 | 0.858 | 10.0 | 1.64 |
| $N_2=N_1+N_{t1}$ | 678 | 0.534 | 6.2 | |
| $N_{\text{test}1}$ | 20 | 0.673 | 8.5 | 1.37 |
| $N_{\text{test}2}$ | 20 | 0.623 | 7.3 | 1.16 |
| $N_3=N_2+N_{t2}$ | 698 | 0.536 | 6.2 | |

| b) E (kcal/mol) | <-1 | <0 | <5 | <10 | <20 | <30 | Total |
|---------------------|------|------|------|------|------|------|-------|
| σ (kcal/mol) | .346 | .329 | .356 | .387 | .417 | .453 | .543 |

Table 6. Final optimized potential parameters ((2) in text). Coulombic term is determined by the fractional atomic charges of the monomer (Table 3).

| Atom pair | A (kcal · Å ⁹ · mole ⁻¹) | B (kcal · Å ³ · mole ⁻¹) |
|-----------|---|---|
| HO-HO | 42.20302 | -6.15294 |
| HO-O | 121.38345 | -23.68087 |
| HO-N | 107.30180 | -9.50863 |
| HO-HN | 1.51723 | -27.20365 |
| O-O | 13 130.35297 | -1.36358 |
| O-N | 30 223.48495 | 275.24918 |
| O-HN | 134.28470 | -48.86516 |
| N-N | 22 039.10274 | 38.21393 |
| N-HN | 1 049.88991 | 11.16646 |
| HN-HN | 4.07493 | -28.57197 |

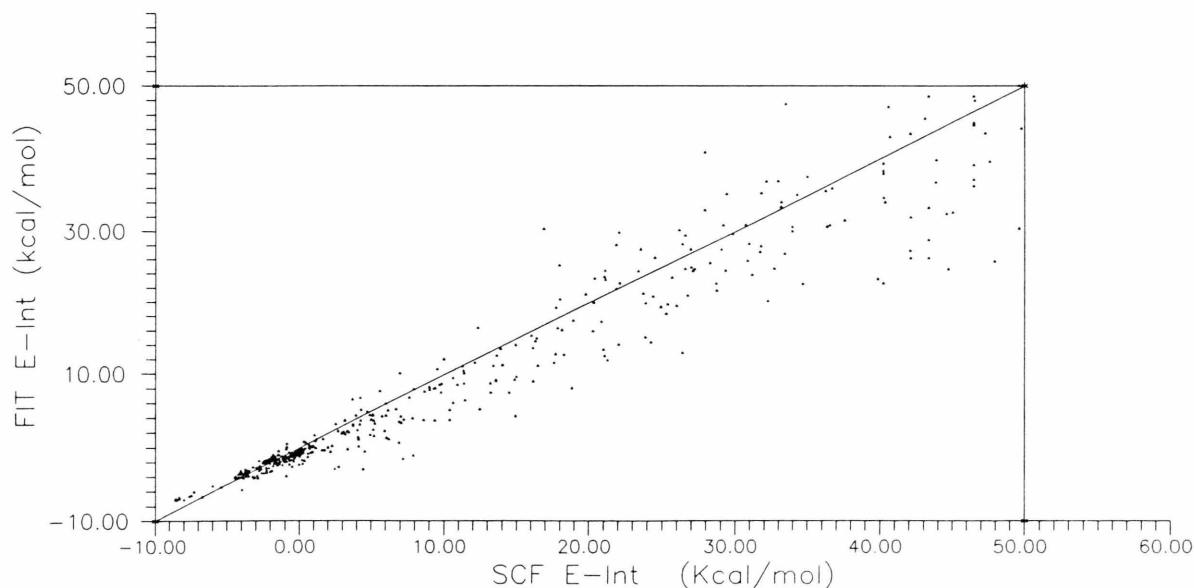


Fig. 3. Comparison of interaction energies: potential fitted values FIT E-int.) versus ab initio calculated (SCF E-int.) for all points in the set.

implied a straight line of unit slope, and the scatter about this line gives a graphical measure of the quality of the function. It is then apparent that the fit is rather good for all important low lying energy points but gets gradually worse, as we move towards the repulsive energy region. This trend was further quantified by a comparison of the standard deviations for different energy ranges (Table 5).

A final test for the quality of the function consisted of a preliminary MC simulation [16] of liquid hydroxylamine at room temperature. This simulation revealed that cyclic dimers amount only to less than 0.5% of the structures in solution, so that the slight misrepresentation of this configuration by our potential curve (Fig. 2) seems to be tolerable and not influential in the condensed phase.

4. Conclusions

The obtained potential function not only is seen to be within statistically acceptable levels of accuracy,

but also to have all physical and chemical features required for a reliable simulation work. However, it should be emphasized here that more work might be needed in the field of deriving accurate potential models for the condensed system. Other phenomena, such as induction and dispersion, could be taken into account in a more systematic way and the inclusion of three- and perhaps four-body terms could become necessary for the successful evaluation of sensitive physical quantities of liquid hydroxylamine in statistical simulation methods.

Acknowledgements

Y.M. would like to thank E. H. S. Anwender for many useful and stimulating discussions. Financial support in form of a fellowship by the Austrian Ministry of Science and Research granted to Y.M. is greatly acknowledged.

- [1] For a review: M. P. Allen and D. J. Tildesley, *Computer Simulation of Liquids*, Oxford University Press, New York 1987.
- [2] G. A. Yeo and T. A. Ford, *J. Mol. Structure* **217**, 307 (1990) and references therein.
- [3] O. Matsuoka, E. Clementi, and M. Yoshimine, *J. Chem. Phys.* **64**, 1351 (1976).
- [4] A. Hinchliffe, D. G. Bounds, M. L. Klein, I. R. McDonald, and R. Righini, *J. Chem. Phys.* **74**, 1211 (1981).
- [5] Y. Tanabe and B. M. Rode, *J. Chem. Soc. Faraday Trans. 2*, **84**, 679 (1988).
- [6] S. Tsunekawa, *J. Phys. Soc. Japan* **33**, 167 (1972).
- [7] N. Tanaka, Y. Hamada, Y. Sugawara, M. Tsuboi, S. Kato, and K. Morokuma, *J. Mol. Spectr.* **99**, 245 (1990).
- [8] N. Tanaka, Y. Hamada, and M. Tsuboi, *Chem. Phys.* **94**, 65 (1985).
- [9] For details and definitions of various basis sets see: *Physical Sciences Data 16: Gaussian Basis Sets for Molecular Calculations* (S. Huzinaga, ed.), Elsevier, Amsterdam 1984.
- [10] M. Krauss and W. J. Stevens, *Ann. Rev. Phys. Chem.* **35**, 357 (1984).
- [11] S. F. Boys and F. Bernardi, *Mol. Phys.* **19**, 553 (1970).
- [12] M. Dupuis, J. D. Watts, H. O. Villar, and G. T. Hurst, *HONDO*, Version 7.0, IBM Technical Report, KGN-169, 1988.
- [13] S. Swaminatham, R. J. Whitehead, E. Guth, and D. L. Beveridge, *J. Amer. Chem. Soc.* **99**, 7817 (1977).
- [14] J. A. Sordo, M. Probst, G. Corongiu, S. Chin, and E. Clementi, *J. Amer. Chem. Soc.* **109**, 1702 (1986).
- [15] W. L. Jorgensen, *J. Chem. Phys.* **70**, 5888 (1979).
- [16] Y. Michopoulos and B. M. Rode, to be published.
- [17] B. M. Rode, *Monatsh. Chem.* **106**, 339 (1975).
- [18] T. H. Dunning, *J. Chem. Phys.* **53**, 2823 (1970).